

THE THEORY OF STEADY STATE SUPER-EDDINGTON WINDS AND ITS APPLICATION TO NOVAE

Nir J. Shaviv

*Canadian Institute for Theoretical Astrophysics, University of Toronto
60 St. George St., Toronto, ON M5S 3H8, Canada*

Submitted to MNRAS

ABSTRACT

We present a model for steady state winds of systems with super-Eddington luminosities. These radiatively driven winds are expected to be optically thick and clumpy as they arise from an instability driven porous atmosphere. The model is then applied to derive the mass loss observed in bright classical novae. The main results are:

- (i) A general relation between the mass loss rate and the total luminosity in super-Eddington systems.
- (ii) A natural explanation to the long duration super-Eddington outflows that are clearly observed in at least two cases (Novae LMC 1988 #1 & FH Serpentis).
- (iii) A quantitative agreement between the observed luminosity evolution which is used to predict both the mass loss and temperature evolution, and their observations.
- (iv) An agreement between the predicted average integrated mass loss of novae as a function of WD mass and its observations.
- (v) A natural explanation for the ‘transition phase’ of novae.
- (vi) Agreement with η Carinae which was used to double check the theory. The prediction for the mass shed in the star’s great eruption agrees with observations to within the measurement error.

Key words: Radiative transfer — hydrodynamics — instabilities — stars: atmospheres — stars: individual LMC 1988 #1, FH Ser, η Carinae — novae, cataclysmic variables

1 INTRODUCTION

The Eddington luminosity is the maximum luminosity allowed for a *stationary* spherical, homogeneous, non-relativistic and fully ionised system. If one allows motion, then a *steady state* super-Eddington configuration generally does not exist unless the system is just marginally super-Eddington or it has a very high mass loss rate. Nevertheless, nature does find a way to construct steady state configurations in which super-Eddington luminosities exist with only a relatively small mass loss rate. This was perhaps best demonstrated with η Carinae’s giant eruption.

η Carinae was clearly super-Eddington during its 20 year long eruption (see for instance the review by Davidson & Humphreys, 1997). Yet, it was shown that the observed mass loss and velocity are inconsistent with a homogeneous solution for the wind (Shaviv, 2000b). Basically, the sonic point obtained from the observed conditions necessarily has to reside too high in the atmosphere, at an optical depth of only ~ 1 to ~ 300 , while the critical point in a homogeneous

atmosphere necessarily has to reside at significantly deeper optical depths. The inconsistency arises because the sonic point and the critical point have to coincide in a steady state solution.

A solution was proposed in which the atmosphere of η Carinae is inhomogeneous, or porous (Shaviv, 2000b). The inhomogeneity is a natural result of the instabilities of atmospheres that are close to the Eddington luminosity (Shaviv, 2000a). The inhomogeneities, or ‘porosity’, reduce the effective opacity and increase the effective Eddington luminosity (Shaviv, 1998).

In this paper, we are interested in understanding the wind generated in cases in which the luminosity is super-Eddington. To do so, it is advantageous to find a class of objects for which better data than for η Car exists. One such class of objects is novae.

Novae are a very good population to analyze in order to understand the behaviour of steady state super-Eddington winds. The main reasons are:

arXiv:astro-ph/0008489v1 30 Aug 2000

(i) The mass and luminosity are better known than for many other objects. For example, although η Carinae was clearly super Eddington, it is not clear by how much it was so: Its mass can be anywhere between $60M_{\odot}$ and $100M_{\odot}$ and its luminosity during the eruption is even less accurately known. The ejected mass could have been between $1M_{\odot}$ and $3M_{\odot}$. This is not accurate enough for our purposes here.

(ii) The opacity where the sonic point is expected to be located is governed by Thomson scattering. In AGB and post-AGB stars that generate strong radiatively driven winds, the opacity is a very sensitive function of the local parameters of the gas at the sonic point. Thus, even though their observed mass and luminosity can be fairly accurately deduced from the observations, the *modified* Eddington parameter which should take into account the opacity of the dust, for example, is not known reasonably well.

(iii) Since the luminosity during the super-Eddington episode of novae eruptions can be significantly above the Eddington limit, the inaccuracy of $\Gamma = L/\mathcal{L}_{\text{Edd}}$ is less critical to the exact value of the mass loss. In objects that shine very close to the Eddington limit for a long duration, with a relatively smaller mass loss rate, the theory cannot give precise predictions. Thus, if for example the winds of the most luminous WR stars arises because the objects are marginally super-Eddington, it would be hard to compare their observations to theory because the accuracy in the determination of $\Gamma - 1$ will be rather poor.

(iv) Novae generally have a ‘bolometric plateau’ in which the bolometric luminosity decreases slowly for a relatively long duration, longer than the dynamical time scale. Therefore, if this luminosity is super-Eddington, then clearly a steady state model for the super-Eddington flow should be constructed. This is clearly the case with two specific novae: Nova LMC 1988 #1 and Nova FH Serpentis. We exclude from the discussion here the very fast novae for which this property is least pronounced.

The fact that the ‘bolometric plateau’ is sometimes observed to be super-Eddington does not presently have any good theoretical explanation. The steady state burning of the post maximum of novae is often predicted to be given or at least approximated by the core-mass luminosity relation (Paczynski, 1970). The classical core-mass luminosity relation increases monotonically with the mass of the WD and saturates at the Eddington limit. It does not yield super-Eddington luminosities. The observations of super-Eddington luminosities over durations much longer than the dynamic time scale, lead us to the hypothesis that bright novae must have a porous atmosphere. A porous atmosphere with a reduced effective opacity will naturally give a core-mass luminosity relation that increases monotonically with mass beyond the classical Eddington limit, providing the arena for steady state super-Eddington winds.

It is these winds which are the subject of this paper. In section 2 we present the ‘wind theory’ for super-Eddington atmospheres. In section 3, we apply the wind theory to two specific novae that were clearly super-Eddington over a long duration, to the nova population in general and to η Carinae and compare the results with observations.

2 THE FUNDAMENTAL STRUCTURE OF SUPER-EDDINGTON WINDS (SEWS)

2.1 Some general considerations

What have we learned from η Carinae? η Car has shown us that an object can be super-Eddington for a duration much longer than the dynamical time scale while driving a wind which is significantly thinner than one should expect in a homogeneous wind solution. When one tries to construct a steady state wind solution, one has to place the sonic point at the critical point—where the net forces on a mass element vanish. If a system is in steady state and super-Eddington at some point, then this point has to reside where alternative means of transporting the energy flux, namely by convection or advection with the flow, become inefficient. This point however, happens relatively deep in the atmosphere, implying that the mass loss $\dot{M} = 4\pi R^2 \rho v_s$ (where v_s is the sound velocity), is very large. In fact, the mass loss rate becomes of order $(L - \mathcal{L}_{\text{Edd}})/v_s^2$ (e.g., Owocki & Gayley, 1997, Shaviv, 2000b). However, if the radius of the system is fixed, then because a minimum energy flux of $\dot{M}GM/R = \dot{M}v_{\text{esc}}^2/2$ (with v_{esc} being the escape velocity) has to be supplied in order to pump the material out of the gravitational well, one obtains that unless $v_s \gtrsim v_{\text{esc}}$, the radiation will not be able to provide the work needed (Owocki & Gayley, 1997). This implies that for the given luminosity and radius of the system, there is no steady state solution. Clearly, the system would try to expand its outer layers (that are driven outward but cannot reach infinity), thereby reducing the escape velocity, until a steady state can be reached.

One would expect that as time progresses, the sonic point of the wind would move monotonically downwards, pushing more and more material upwards thereby expanding the atmosphere and accelerating more mass until all the available luminosity would be used-up to pump material out of the well. η Car would have appeared as a faint object with high mass loss at low velocities. In other words, observations of η Car suggest that down to the optical depth of at most $\lesssim 300$, which is the deepest that the sonic point could be located (Shaviv, 2000b), the total mass is $\lesssim 0.02M_{\odot}$, implying that this part of the envelope should have been in steady state for time scales longer than $\lesssim 3$ months. This steady state is inconsistent with η Car trying to reach an equilibrium in which most of the radiation is used up to accelerate a very large amount of mass to low velocities, the star has been markedly super-Eddington for a long duration without accelerating more and more mass at lower velocities.

We will soon show that novae, at least during their ‘bolometric plateau’ defy the Eddington limit. In some cases at least, a steady state super-Eddington configuration is reached in which the kinetic energy in the flow plus the rate in which gravitational energy is pumped is only a small or moderate fraction of the total radiative energy flux at the base of the wind. This too is inconsistent with a sonic point that lays deep inside the atmosphere.

So, how did η Car circumvent its bloating up? It was proposed by Shaviv (2000b) that the solution to the problem is having a porous atmosphere. In such an atmosphere, density perturbations naturally reduce the effective opacity κ_{eff} (Shaviv, 1998). Consequently, the radiative force is decreased and the effective Eddington limit is increased to:

$$\mathcal{L}_{\text{eff}} = \frac{\kappa_0}{\kappa_{\text{eff}}} \mathcal{L}_{\text{Edd}} > \mathcal{L}_{\text{Edd}}, \quad (1)$$

where κ_0 is the microscopic opacity. When $\kappa_0 = \kappa_{\text{Thomson}}$, the Eddington limit \mathcal{L}_{Edd} corresponds to the *classical* Eddington limit. In most other case, where the microscopic opacity κ_0 is larger, \mathcal{L}_{Edd} corresponds to the lowered *modified* Eddington luminosity. In the rest of this work, we shall not explicitly state whether the Eddington limit is ‘classical’ or ‘modified’. The distinction should be made according to the underlying microscopic opacity, which will be that of Thomson scattering in the specific cases studied here. We shall however make the important distinction with the ‘effective’ Eddington luminosity which is the effective value in a non-homogeneous system.

A mechanism which converts the homogeneous layers into inhomogeneous was suggested by Shaviv (2000a). It is demonstrated that as the radiative flux through the atmospheres surpasses a critical Eddington parameter of $\Gamma_{\text{crit}} \sim 0.6 - 0.8$ (the exact numerical value depends on the boundary conditions), the atmosphere becomes unstable to at least two different instabilities, one of which operates on a dynamical time scale. Consequently, as the radiative flux approaches the Eddington limit and surpasses it, the radiation triggers the transition of the atmosphere from a homogeneous one to an inhomogeneous one. The inhomogeneities increase the effective Eddington limit thereby functionally keeping the radiation flux at a sub-Eddington level; namely, even if $\Gamma > 1$, the optically thick regions experience a $\Gamma_{\text{eff}} < 1$. Other instabilities that operate in more complex environments could too be important and contribute to this transition. For example, *s*-mode instabilities (Glatzel & Kiriakidis, 1993) or the instability of dynamically detached outer layers (Stothers & Chin, 1993) operate under more complex opacity laws. The instability of ‘photon bubbles’ appears when strong magnetic fields are present (Arons, 1992). In principle, since the adiabatic index approaches the critical value of 4/3 for instability as the Eddington limit is approached, many mechanisms which are otherwise unimportant do become important.

The ‘porosity’ reduces the effective opacity only as long as the perturbations are optically thick. Therefore, a wind will necessarily be generated from the regions in which the perturbations become optically thin, since from these regions upwards the effective opacity will be the normal ‘microscopic’ one and the effective Eddington limit will return to be the classical one.

The details of the geometry (or inhomogeneities) of the regions depend on the instability at play, and for example can be in the form of ‘chimneys’ or ‘photon bubbles’. The lowered opacity is achieved by funneling the radiation through regions with a much lower than average density. These regions can be super-Eddington even when the mean Γ parameter is smaller than unity. In such cases, mass should be driven in the super-Eddington ‘chimneys’ of lower density. These atmospheres are then expected to be very dynamic. Once any accelerated mass element reaches the optically thin part of the atmosphere, it will start to experience an average force that is at a sub-Eddington value and the mass flow will stagnate, probably forming something which looks like ‘geysers’. (It is very unlikely that the escape velocity will be attainable in the ‘chimneys’ since shocks would probably limit the flow to velocities not much larger than

the speed of sound). A wind could then be generated in the optically thin part of the atmosphere through the standard line driving mechanism (Castor et al., 1975, or for example Pauldrach et al., 1986 and references therein), with the notable consideration that the base of the wind is clumpy.

When $\Gamma > 1$ on the other hand, a continuum driven wind has to be generated. The reason is clear. Since the perturbations have to be optically thick to affect (and reduce) the opacity, at a low enough optical depth one would expect to return back to a super-Eddington flow. What is this optical depth? If we climb up the thick yet porous atmosphere, since it is effectively sub-Eddington, its average density will decay exponentially with height. At some point, the density will be low enough that a typical perturbation ‘element’ becomes optically thin. Since the perturbations are expected to be of order a scale height in size (Shaviv, 2000a), this depth would be where a scale height has an optical *width* of order unity*. Beyond this point, the typical perturbation on scales of order the a scale height cannot reduce the opacity. This is the place where the sonic point should be located.

More specifically, if the flux corresponds to an Eddington parameter Γ , then the optical depth at which perturbations cannot reduce the effective Eddington parameter to unity, should scale with $\Gamma - 1$. The reason is that the decrease of the luminosity by the effective opacity should be proportional to the deviation of the actual luminosity from the Eddington one. Namely, when close to the Eddington limit, a blob with the same geometry needs a smaller density fluctuation and with it a smaller change in the opacity, to reduce the effective opacity by the amount needed to become Eddington. Thus, when closer to the Eddington limit, the sonic point can sit higher in the atmosphere.

2.2 The Structure of a Steady SEW

The above considerations lead us to propose the following structure of a super-Eddington wind (hereafter SEW). Consider Fig. 1 for the proposed structure of a super-Eddington atmosphere (one with $L_{\text{tot}} > \mathcal{L}_{\text{Edd}}$) and the SEW that it generates. Four main regions can be identified in the atmosphere and they are:

- Region A: A Convective envelope – where the density is sufficiently high such that the excess flux above the Eddington luminosity is advected using convection. The radiative luminosity left is below the classical Eddington limit: $L_{\text{rad}} < \mathcal{L}_{\text{Edd}} < L_{\text{tot}}$. It was shown by Joss, Salpeter & Ostriker (1973) that convection is always excited before the Eddington limit is reached. Thus, if the density is high enough and the total flux is super-Eddington, this region has to exist.
- Region B: A zone with lower densities, in which convection becomes inefficient. Instabilities render the atmosphere inhomogeneous, thus facilitating the transfer of flux

* Note that if the atmosphere is static and therefore has an exponential density profile, this location would also correspond to the place at which the optical *depth* is of order unity. Since a thick wind is expected to form, the physical depth where the optical *width* of a scale height is of order unity does not correspond to the physical location where the optical *depth* is of order unity.

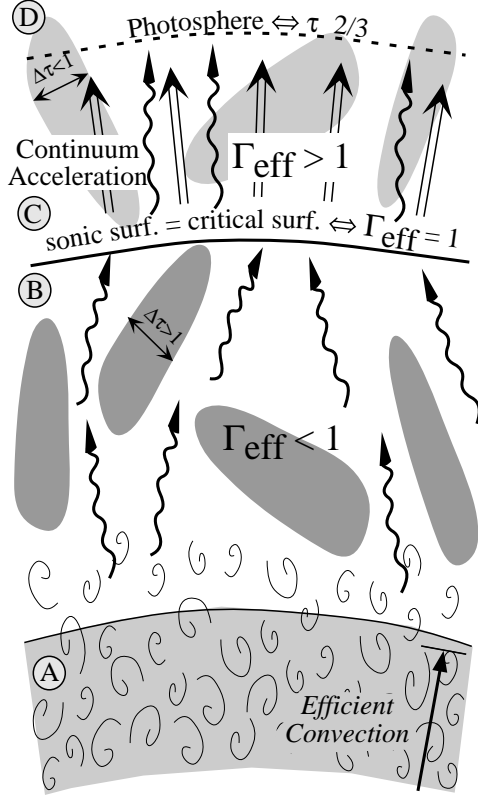


Figure 1. The proposed structure of a super-Eddington atmosphere (one with $L_{\text{tot}} > \mathcal{L}_{\text{Edd}}$) and the wind that it generates. The four regions, which are described in detail in the text, are: Region (A) A Convective envelope in which the radiation is sub-Eddington – $L_{\text{rad}} < \mathcal{L}_{\text{Edd}} < L_{\text{tot}}$. Region (B) A porous atmosphere in which the effective Eddington luminosity is larger than the classical Eddington luminosity: $\mathcal{L}_{\text{Edd}} < L_{\text{rad}} = L_{\text{tot}} < \mathcal{L}_{\text{eff}}$. Region (C) of an optically thick, continuum driven wind, where perturbations are optically thin and the effective Eddington limit tends to the classical value. Region (D) of a photosphere and above.

without exerting as much force. The effective Eddington luminosity is larger than the classical Eddington luminosity. $\mathcal{L}_{\text{Edd}} < L_{\text{rad}} = L_{\text{tot}} < \mathcal{L}_{\text{eff}}$. η Car has shown us that the existence of this region allows for the steady state outflow during its 20 year long eruption (Shaviv, 2000b).

- Region C: A region in which the effect of the inhomogeneities disappears and the luminosity is again super-Eddington. When perturbations arising from the instabilities, which are expected to be of order the scale height in size, become transparent, the effective opacity tends to the microscopic value and the effective Eddington limit tends to the classical value. At the transition between (B) and (C), the effective Eddington is equal to the total luminosity. This critical point is also the sonic point in a steady state wind. Above the transition surface, $L_{\text{tot}} > \mathcal{L}_{\text{eff}} \rightarrow \mathcal{L}_{\text{Edd}}$ and we have a super sonic wind. This wind is expected to be optically thick.

- Region D: The photosphere and above. Since the wind is generally thick, the transition between regions (C) and (D) is far above the sonic surface.

The pressure scale height of the atmosphere below the sonic point, where the velocity is small, is:

$$h = \frac{\nu v_s^2}{g(1 - \Gamma_{\text{eff}})} \quad (2)$$

In isothermal or adiabatic (convective) atmospheres, ν is respectively $1/\gamma$ and 1. In a radiative atmosphere, ν depends on the opacity law, but in any case, we always expect $\nu \sim \mathcal{O}(1)$. The effective Eddington parameter Γ_{eff} stays below unity even if $\Gamma > 1$, as we have learned from η Car (Shaviv, 2000b).

The optical width of the scale height at the sonic point is $\Delta\tau_* \approx \rho_* \kappa h$, giving

$$\rho_* = \frac{\Delta\tau_*}{\kappa h} = \frac{\Delta\tau_* G M_* (1 - \Gamma_{\text{eff}})}{\kappa \nu v_s^2 R_*^2}. \quad (3)$$

All quantities with the index $*$ relate to the sonic point (and also the critical point), which can be considered as the hydrostatic radius of the star. The mass loss should be $\dot{M} = A_{\text{eff}} \rho_* v_s$. A_{eff} is the effective area through which mass is lost. It is smaller than $4\pi R_*^2$ because only some fraction f is super-Eddington, while a fraction $1 - f$ is covered with high density/low luminosity patches. Thus,

$$\begin{aligned} \dot{M} &= 4\pi R_*^2 f \rho_* v_s = \frac{f \Delta\tau_* 4\pi G M_* (1 - \Gamma_{\text{eff}})}{\kappa \nu v_s} \\ &= \frac{(1 - \Gamma_{\text{eff}})(\Gamma - 1)\tau_0 \mathcal{L}_{\text{Edd}}}{\nu c v_s} \equiv \mathcal{W}(\Gamma) \frac{L_{\text{tot}} - \mathcal{L}_{\text{Edd}}}{c v_s}, \end{aligned} \quad (4)$$

where

$$\mathcal{W}(\Gamma) = \frac{1 - \Gamma_{\text{eff}}}{\nu} \tau_0 \gtrsim \mathcal{O}(1). \quad (5)$$

Note again that \mathcal{L}_{Edd} becomes the modified Eddington luminosity if the underlying opacity is not that of Thomson scattering. Eq. (5) is the basic result of the present theory. We have used the expected scaling that $\Delta\tau_* = (\Gamma - 1)\tau_0$ with τ_0 expected to be a constant of order of unity, or perhaps somewhat larger, depending on the efficiency at which the effective opacity can be reduced (the smaller the efficiency, the larger will τ_0 be). The other parameters that enter the function $\mathcal{W}(\Gamma)$ are also expected to be of order unity and weak functions of Γ . Hence, we assume for simplicity that $\mathcal{W}(\Gamma)$ is a constant of order unity, or perhaps somewhat larger. It is only with a more elaborate simulation or with more accurate and careful observations, that a more accurate functional form can be deduced. For the meantime, we will have to settle with this simplifying yet reasonable assumption.

We will show in the rest of the paper that eq. (5) provides an explanation to the mass loss from bright classical novae as well as from η Carinae and allows us to connect between the observed luminosity and mass loss rate, a relation which hitherto did not exist for super-Eddington systems.

2.3 High Load winds

Unlike normal stellar winds, the thick winds that are formed in the super-Eddington flows not only have a high mass momentum relative to the photon momentum, which is expected in any thick wind, but more importantly, the kinetic energy flux can be comparable to the radiative luminosity. It

also inadvertently implies that the rate of gravitational energy being ‘pumped’ into the outflowing matter is also comparable. Consequently, the luminosity appearing in eq. (5) is not the observed luminosity at infinity. Instead, it is:

$$\begin{aligned} L_\star \approx L_{\text{tot}} &= L_\infty + \dot{M} \left(\frac{v_\infty^2}{2} + \frac{GM}{r_\star} \right) \\ &= L_\infty + \frac{\dot{M}}{2} (v_\infty^2 + v_{\text{esc}}^2). \end{aligned} \quad (6)$$

(The approximation neglects the kinetic energy at the sonic points, i.e., assuming that $v_s^2 \ll v_{\text{esc}}^2$ which gives $L_{\text{tot}} \approx L_\star$). The effect of a lowered observed luminosity was coined ‘photon tiring’ by Owocki & Gayley (1997), who solved for the behaviour of the evolution of the wind. Their solution related the variables L_∞ , L_\star , \dot{M} , v_∞^2 and v_{esc}^2 . The basic equations are the equations of continuity, momentum conservation and energy conservations:

$$\dot{M} = \text{const} = 4\pi r^2 v \rho \quad (7)$$

$$\frac{1}{2} \frac{dv^2}{dr} = \frac{-GM_\star(1 - \Gamma(r))}{r} \quad (8)$$

$$L(r) = L_\star - \dot{M} \left[\frac{v^2}{2} + \frac{GM_\star}{R_\star} - \frac{GM_\star}{r} \right] \quad (9)$$

$\Gamma(r)$ is the ratio between the Luminosity $L(r)$ and the local modified Eddington luminosity \mathcal{L}_{Edd} which we assumed to be constant, since the opacity is assumed to be given by the Thomson scattering. The solution to this set of equations, after neglecting the speed of sound at the base of the wind, is (Owocki & Gayley, 1997):

$$\begin{aligned} w \equiv \frac{v^2}{v_{\text{esc}}^2} &= -x + \frac{\Gamma_\star}{\tilde{m}} (1 - \exp(-\tilde{m}x)) \Big|_{r \rightarrow \infty} \\ &= -1 + \frac{\Gamma_\star}{\tilde{m}} (1 - \exp(-\tilde{m})), \end{aligned} \quad (10)$$

where x is defined as $1 - R_\star/r$. R_\star is the radius of the sonic point of the wind and can be described as the ‘hydrostatic’ radius of the star. Below it, the envelope is expanding with a subsonic speed. \tilde{m} is defined as $\dot{M}GM_\star/\mathcal{L}_{\text{Edd}}R_\star$. It is a slightly different definition for the ‘photon tiring number’ than the original definition of m by Owocki & Gayley (1997). The two are related through $\tilde{m} = \Gamma_\star m$.

Using the wind model developed here (eq. 5), we can close the relation between \dot{M} (or \tilde{m}) and the luminosity of the star:

$$\tilde{m} = \frac{1}{2} \frac{v_{\text{esc}}^2 \dot{M}}{\mathcal{L}_{\text{Edd}}} = \frac{1}{2} \frac{v_{\text{esc}}^2}{v_s c} \mathcal{W}(\Gamma_0 - 1) \equiv \tilde{W}(\Gamma_0 - 1), \quad (11)$$

where \tilde{W} is the ‘scaled’ wind parameter. This is a dimensionless version of eq. (5) – the basic mass-loss luminosity relation of SEWs.

For given Γ_\star , \mathcal{L}_{Edd} and R_\star (or v_{esc}^2), we can now calculate \tilde{m} (or \dot{M}), and from it calculate w_∞ (or v_∞^2) and Γ_∞ . To get the latter, we substitute the energy conservation equation into the equation for w to get:

$$\Gamma_\infty = \Gamma_\star \exp(-\tilde{m}). \quad (12)$$

In order to compare with observations, we need to translate L_∞ , \dot{M} and v_∞ , into T_{eff} . This is done using a steady state optically thick wind model. When integrated upwards, a photosphere should be obtained where the optical depth is

of the order of $2/3^\dagger$. The general case is far from trivial because the opacity is $\sim \sqrt{\kappa_{sc}\kappa_{ab}}$ where κ_{ab} is the absorptive opacity which is generally much smaller than the scattering opacity. The simplest approximation is first to assume that the opacity is that of Thomson scattering. This was done when the original steady state optically thick wind explanation to novae was proposed (Bath & Shaviv, 1976). It yields an effective temperature that satisfies the following equation:

$$\begin{aligned} \log \left(\frac{\dot{M}}{\text{gr s}^{-1}} \right) &= 21.0 - 2.0 \log \left(\frac{T_{\text{eff}}}{10^4 \text{ }^\circ\text{K}} \right) \\ &+ \log \left(\frac{v}{10^8 \text{ cm s}^{-1}} \right) + 0.5 \log \left(\frac{L_\infty}{10^{38} \text{ erg s}^{-1}} \right). \end{aligned} \quad (13)$$

In reality though, the absorption opacity is lower and the photosphere is deeper in the wind, where the temperature is higher. Thus, a temperature estimate based on eq. (14) will be adequate only when we use an effective temperature that is defined through $\sigma T_e^4 \equiv L/4\pi R^2$, where R is the radius where the optical depth for the continuum becomes $2/3$. This temperature is used, for example, in the analysis by Schwarz et al. (1998). If a real colour temperature is needed (such as by comparison to a Planckian spectrum), then a more extended analysis, as was carried out by Bath (1978) is needed. Since we do not require a very accurate mass loss temperature relation (as the measurement error from observations is much larger anyway), a simple fit to Bath’s results is sufficient. One obtains that for $T \gtrsim 6000^\circ\text{K}$, the relation is:

$$\begin{aligned} \log \left(\frac{\dot{M}}{\text{gr s}^{-1}} \right) &= 22.3 - 1.48 \log \left(\frac{T_{\text{colour}}}{10^4 \text{ }^\circ\text{K}} \right) \\ &+ \log \left(\frac{v}{10^8 \text{ cm s}^{-1}} \right) + 0.65 \log \left(\frac{L_\infty}{10^{38} \text{ erg s}^{-1}} \right). \end{aligned} \quad (14)$$

It provides an estimate to $\log \dot{M}$ that is better than 0.1, which is more than sufficient for our purpose here.

The last relation that we need in order to close the set of equations is to find the exact value of v_s at the base of the wind. For that, we need the temperature at the base of the wind. For simplicity, we assume that the velocity is constant and equal to the terminal value; in other words, most of the acceleration takes place deep in the optically thick part. This is valid as long as $r_{\text{ph}} \gg R_\star$. Under these conditions, the temperature at the bottom can be estimated as:

$$T_\star \approx T_{\text{ph}} \left(\frac{r_{\text{ph}}}{R_\star} \right)^{3/4} \left(\frac{\Gamma_\star}{\Gamma_\infty} \right)^{1/4}. \quad (15)$$

The speed of sound at the bottom is $\propto \sqrt{T}$, thus, the overall variation of v_s over the range of physical parameters that will soon be found to be modest in novae.

The set of dimensionless equations (10, 11, 12, 15, and 14 or 15) can now be used to obtain from Γ_\star and \tilde{W} the entire set of parameters in the system: v_∞ , \dot{M} , Γ_∞ , T , R_\star etc. Those are seen in the contour plots depicted in Fig. 2 for a $1M_\odot$ system.

[†] The photosphere in a spherical geometry does not sit at exactly $\tau = 2/3$, though we assume so for simplicity.

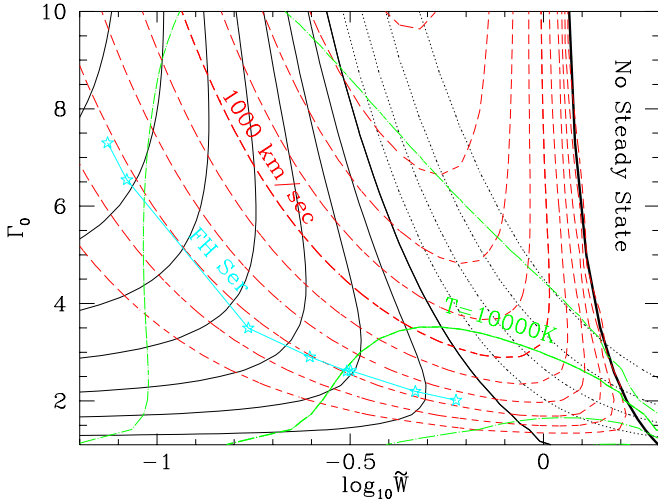


Figure 2. The evolution of FH Ser in the Γ_* - \tilde{W} plane. Γ_* is the Eddington parameter at the base of the wind while \tilde{W} is a dimensionless parameter describing the relative ‘load’ of the wind: $\tilde{W} \equiv W v_{\text{esc}}^2 / 2v_s c$. Larger \tilde{W} 's imply a smaller base radius. The additional lines are iso-contours of the observed Eddington parameter Γ_∞ (the solid lines for $\Gamma_\infty \geq 1$ are spaced at 0.2 dex, and dotted spaced linearly at 0.2 intervals for $\Gamma_\infty < 1$), v_∞ (short-long dashed lines spaced at intervals of 100 km/sec, higher are larger) and the colour temperature of the photosphere T_{ph} (dot-dashed lines spaced at 2500°K, lower lines are hotter). The evolution from top left to bottom right was calculated by integrating the following equations: (a) The wind model to relate \dot{M} to Γ_* (given in this work), (b) The temperature mass loss relation (given by Bath 1978), and (c) Relations between the observed parameters and the parameters at the base of the wind (given by Owocki & Gayley 1997). The stars are the values obtained at different days from the data of Friedjung (1987)

3 APPLICATION OF THE SEW THEORY

We now proceed to apply the SEW theory to systems that clearly exhibited super-Eddington outflows over dynamically long durations.

3.1 Two super-Eddington nova

Although many novae display super-Eddington luminosities for at least short periods, it is often difficult to unequivocally show that a particular nova was indeed super-Eddington for a *long* duration, even if it was[‡]. The reason is that during the ‘bolometric plateau’ that a nova exhibits, the luminosity can be close to the Eddington limit (from either above or below it) such that even small uncertainties in distance and luminosity can hide the true nature of the flow. Moreover, since the wavelength of maximum emission shifts to the UV during the ‘bolometric plateau’, as the temperature increases, it is difficult to acquire accurate bolometric luminosities from Earth based observations. Our insistence of obtaining good data results with having only two clear cases in which long duration super-Eddington flows were

[‡] On average, the absolute magnitude M_B of a classical novae of which the WD mass $\gtrsim 0.5M_\odot$, peaks at a super-Eddington luminosity (Livio, 1992).

observed and have good enough data. The two cases are Nova LMC 1988 #1 and Nova FH Serpentis. Other cases such as V1500 Cygni are not as clear cut, even though one would suspect that long duration SEWs could have been present. In V1500 Cygni, the nova was observed to shine at significantly super-Eddington luminosities for a few days after the eruption, and when observed again on day 100, it was 2/3 of Eddington. Thus, there is no clear indication for the duration of the super-Eddington episode, only a lower limit. Another recent example is Nova LMC 1991, which was observed to be super-Eddington for two weeks (Schwarz et al., 2000), reaching a truly impressive luminosity as high as $2.6 \pm 0.3 \times 10^{39} \text{ ergs}^{-1}$! As we shall soon see, both V1500 Cygni and LMC 1991 were classified as very fast novae and hence are marginally useful candidates for a *steady state* analysis. Another nova, V1974 Cygni 1992, had very beautiful bolometric observations (Shore et al., 1994) which could have been potentially very useful for the analysis done here. Unfortunately, the distance uncertainty of 1.8 to 3.2 kpc (Paresce et al., 1995) corresponds to more than a factor of 3 uncertainty in the bolometric luminosity, which is too large.

3.1.1 Nova LMC 1988 #1

Nova LMC 1988 #1 occurred, as the name suggests, in the LMC. Thus, its distance is known more accurately than galactic novae. This distance, coupled to an extensive multi-wavelength campaign by Schwarz et al. (1998), resulted with their rather accurate finding that Nova LMC 1988 #1 had an average bolometric luminosity of $(3.0 \pm 0.3) \times 10^{38} \text{ erg s}^{-1}$ during the first 45 days after visual maximum. By considering that the maximum mass a WD can have is $1.4 M_\odot$, Schwarz et al. (1998) concluded that the nova had to be super-Eddington for the long duration. We use their data and results for the analysis. This includes the evolution of the bolometric luminosity and the effective temperature (as opposed to a colour temperature).

3.1.2 Nova FH Serpentis

Nova FH Serpentis is less clear than Nova LMC 1988 #1. Specifically, an accurate distance determination was obtained only after using the HST measurement of the expanding ejecta (Gill & O’Brien, 2000). The reddening which is inaccurately known (and is probably in the range $E(B-V) = 0.64 \pm 0.16$, della Valle et al., 1997) then remains as the main source of error in the bolometric luminosity determination. If we take the determination of the possible range for the bolometric luminosity by Duerbeck (1992) and della Valle et al. (1997) and correct for the somewhat larger distance determined by Gill & O’Brien (2000), we find that the bolometric luminosity on day 6.4, when the first UV measurement was taken, is $M_{\text{bol}} = -7.5 \pm 0.2$, namely, L must have been more than $2.5 \times 10^{38} \text{ erg s}^{-1}$.

Further, since the total mass ejected has a lower bound of $5 \times 10^{-5} M_\odot$, and is probably more of the order of $2 \times 10^{-4} M_\odot$, we should take the kinetic energy of the outflow into account. Since the ejecta is moving at about 500 km s^{-1} (Gill & O’Brien, 2000), the ejecta has a minimum kinetic energy of $2.5 \times 10^{44} \text{ erg}$. A lower estimate to

the contribution of the kinetic energy to the total flux at the base of the wind would be to divide the kinetic energy uniformly over the duration of the bolometric plateau that lasted about 45 days. This gives a minimum contribution of $L_{\text{kin,min}} = 6.5 \times 10^{37} \text{ erg s}^{-1}$. Since the total mass loss is probably higher than $5 \times 10^{-5} M_{\odot}$ and since the mass loss rate was likely to be higher than average when the luminosity was higher than the average luminosity, it is likely that $L_{\text{kin}} > L_{\text{kin,min}}$ at day 6.4. When we add the kinetic energy to the observed bolometric luminosity at day 6.4, we find that L_{tot} at the base of the wind must have been at least $3.1 \times 10^{38} \text{ erg s}^{-1}$. Clearly, even if the mass of the WD is large (which is inconsistent with the eruption not being a very fast nova), the luminosities are super-Eddington. The fact that the kinetic energy necessarily implies that the nova was super-Eddington (at the base of the wind) was already pointed out by Friedjung (1987) who did not have observations on the mass ejected but instead used photospheric constraints on \dot{m} . Here, we have reached the same conclusion without resorting to the photospheric analysis. This could be done due to the better distance measurements (which are within the error but on the large side of previous estimates), and better reddening measurements of della Valle et al. (1997).

We use the data of Friedjung (1987, also in Friedjung, 1989) for the temperature and luminosity behaviour. These data are based on the UV measurements by Gallagher & Code (1974) but which include the integrated flux that falls outside the UV range observed by Gallagher & Code assuming a black body distribution[§]. We correct the luminosities to include the better distance determination by Gill & O'brian (2000).

3.2 Is steady state model appropriate for the 'bolometric plateau' of novae?

A steady state model is probably appropriate for two reasons:

(i) Circumstantial evidence: Kato & Hachisu 1994 compared their steady state model for winds to the results of a dynamical evolution of Prialnik (1986) and found relatively good agreement, implying that a steady state solution is valid for most of the nova evolution.

(ii) Physical reasons: A wind with a terminal velocity of v_{∞} originates from a typical radius r_{\star} that has an escape velocity of order v_{∞} . Two conditions should therefore be satisfied for the wind to be in a steady state. First, the sub-sonic region beneath the base of the wind should be acoustically connected on time scales shorter than the typical evolution time of the system. Namely:

$$t_{\text{sub-sonic}} \approx \frac{r_{\star}}{v_s} \ll t_{\text{evolution}}. \quad (16)$$

The second criterion is that the time it takes the accelerated material to reach the photosphere is shorter than the time at question:

[§] Note that when taking this extra flux outside the observed UV range, the slow increase followed by a decrease in bolometric luminosity, as described by Gallagher & Code (1974), turn into a slow decrease of the bolometric luminosity.

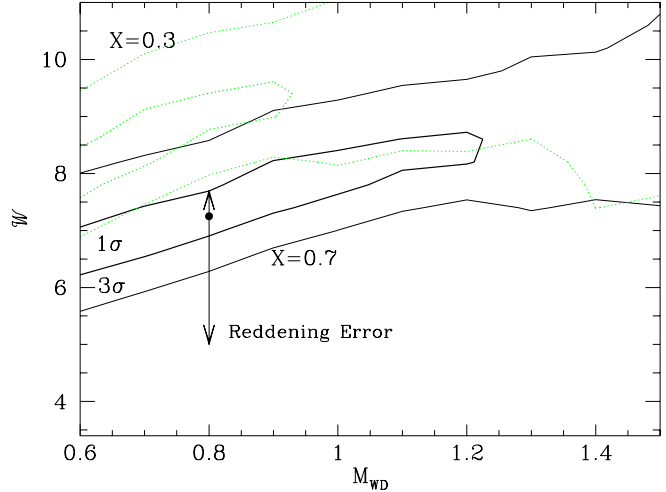


Figure 3. The χ^2 fit of the predicted temperature (from the luminosity and wind theory) to the observed temperature variations of Nova FH Serpentis, for two values of the Hydrogen mass fraction X . The 1 and 3 σ statistical variation contours are marked in the $\mathcal{W} - M_{\text{WD}}$ plane. Good fits are obtained for reasonable parameters. A χ^2 of 4.2 is obtained for $8 - 2 = 6$ degrees of freedom. The systematic errors are large and arise from the inaccurate knowledge of M_{WD} , X and the reddening to Nova FH Serpentis. The limit on the systematic variation of the latter is given by the arrows.

$$t_{\text{super-sonic}} \approx \frac{r_{\text{ph}}}{v_{\infty}} \ll t_{\text{evolution}}, \quad (17)$$

where $t_{\text{evolution}}$ is the typical time scale for changes in the system. Both Nova FH Serpentis and Nova LMC 1988 #1 satisfy both requirements from days 4 and 2 respectively. Thus, a steady state solution for the objects ought to be found for $t_{\text{evolution}} \approx \text{month}$. As previously mentioned, Novae V1500 Cygni and LMC 1991 do not satisfy the required conditions – they are very fast novae that evolve dramatically on a time scale of days, so a steady state wind cannot be assumed in their analysis.

3.3 Application to Nova FH Serpentis

Using the described method of analysis, we fit for the data of Friedjung (1987). We allow \mathcal{W} and M_{\star} to be free parameters (with a hydrogen fraction X , and therefore an $\mathcal{L}_{\text{Edd}}/M_{\star}$ ratio fixed) and find for the best fitting model.

The results for $X = 0.3, 0.7$ are depicted in Fig. 3. We find that the possible $1 - \sigma$ range for \mathcal{W} is about 6 to 9.5. If we allow larger statistical variation of $3 - \sigma$ then the value of \mathcal{W} can range from 5.5 to about 11 (if we restrict ourselves to a reasonable WD mass range between 0.6 and 1.0 solar masses).

An additional systematic error arises from the inaccuracy of the derived reddening to Nova FH Serpentis. This uncertainty is portrayed by the error which could increase or decrease the derived \mathcal{W} by roughly +0.5 or -2 respectively.

The fit to the observed temperature evolution for the best fit for the nominal values of $X = 0.7$ and $M_{\text{WD}} = 0.8 M_{\odot}$ is described in Fig. 4. Good agreement between the predicted temperature using the SEW theory and the ob-

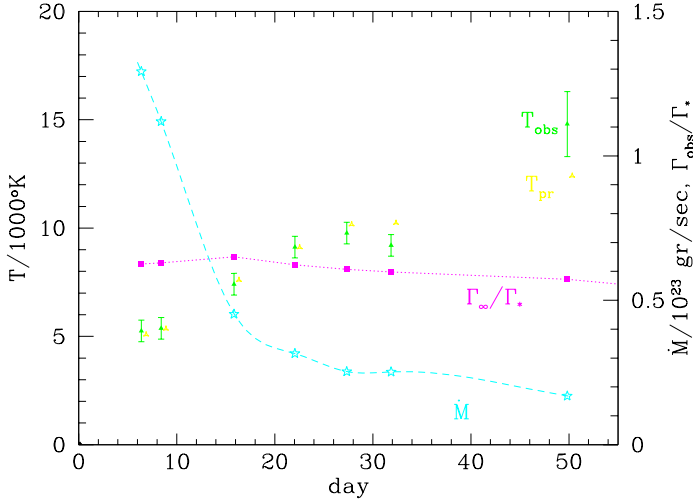


Figure 4. The observed temperature behaviour T_{obs} of Nova FH Serpentis (filled triangles, taken from Friedjung 1987) as compared with the predicted temperature behaviour T_{pr} from the observed luminosity and wind model (open triangles, slightly offset to the right), for the best fit model assuming $M_{\text{WD}} = 0.8M_{\odot}$ and $X = 0.70$. The additional plots are of the mass loss (the stars and dashed line). The mass loss integrates to $8 \times 10^{-5}M_{\odot}$. Finally we plot as filled squares the ratio of Γ_{∞} to Γ_{\star} . Apparently, about 40% of the original radiative luminosity at the base of the wind is used-up under these parameters to accelerate the wind and compensate for its potential energy.

served colour temperature can be obtained, clearly demonstrating that the theory is consistent.

The temporal evolution of the observed luminosity, as given in the same figure, can be integrated to obtain a total mass loss of $8 \times 10^{-5}M_{\odot}$. The main source of uncertainty in this figure is again the reddening which could increase or decrease the mass loss by about +10% and -30% respectively. This result is completely consistent with the observations that range $(2 - 20) \times 10^{-5}M_{\odot}$ (Hack et al., 1993, Gill & O’Brien, 2000).

An important point which should be considered is that the wind is likely to be clumpy, a fact which the analysis thus far did not take into account. In the region around the sonic point, the optical depth of typical clumps is expected to be of order unity. Above this point, typical clumps are therefore expected to be optically thin. Thus, the main effect of the clumpiness is to increase the effective absorptive opacity (since one will then obtain that $\kappa_{\text{abs}} \propto \sqrt{\langle \rho^2 \rangle} > \sqrt{\langle \rho \rangle^2}$). The effective opacity which is proportional to the geometric mean of the scattering and absorptive opacities will increase as $\sqrt{\delta}$ were δ is a clumpiness parameter:

$$\delta \equiv \sqrt{\langle \rho^2 \rangle / \langle \rho \rangle^2}. \quad (18)$$

Moreover, from Bath & Shaviv (1976) we have that for a fixed temperature, outflow velocity and luminosity, the inferred mass loss rate is proportional to $\kappa^{-3/2}$. Thus, one would over estimate \mathcal{W} by roughly a factor of $\delta^{3/4}$.

We do not know what the value of δ should be. A rough guesstimate would be to take the value found in another type of system in which strong optically thick winds are observed, namely, WR stars. In binary systems in which one

of the stars is a WR, several measurements of the mass loss in the winds can be performed. Some (which are usually the more difficult ones) measure the actual mass loss \dot{m} (for example, using scattering induced polarizations or measurement of \dot{P}) while others measure $\dot{m}\delta$ (for example, using radio measurements of the free-free emission). In the case of V444 Cygni, a value of $\delta \approx 3$ is obtained (St.-Louis et al., 1993). If we adopt this value as a typical one, then the inferred range of $\mathcal{W}\delta^{3/4}$ is 3.5 - 11.5, which corresponds to $\mathcal{W} = 1.5 - 5$. For comparison, we expect from the SEW theory to have \mathcal{W} to be somewhat larger than unity, and indeed, so is found.

3.4 Application to Nova LMC 1988 #1

Nova LMC 1988 #1 has better data than Nova FH Serpentis in several respects. First, the absolute luminosity is better known. Second, the temperature obtained by Schwarz et al. (1998) is an effective temperature and not the colour temperature. Consequently, the analysis does not depend on the absorptive opacity and therefore the clumpiness of the wind. The main draw back however, is that Nova LMC 1988 #1 does not have adequate measurements of the evolution of the velocity of the outflow. The velocity of $1800 \pm 200 \text{ km s}^{-1}$ adopted by Schwarz et al. (1998) is based on the measurements of optical emission lines that are also consistent with the subsequent observations of ‘Orion’ emission lines when the nova was optically thin. There are no available records to velocities derived from the principal (absorptive) spectrum.

An important question should be raised. Is the velocity of the the photospheric material given by the velocity of the diffuse enhanced spectrum or by the principal spectrum? The answer is probably the latter. Irrespective of the theoretical argumentation for which spectrum is formed closer to the photosphere, the circumstantial evidence points to the principal spectrum. This is because the velocities obtained from the principal spectrum are similar to those obtained by measurements of the nebular expansion years after the eruption. Namely, the principal spectrum provides the velocity of the bulk of the material while the diffuse enhanced spectrum probably gives the velocity of the small amount of material that is initially injected at high speeds. In Nova FH Serpentis for example, the principal spectrum gives velocities in the range 670 to 770 km s^{-1} . The diffuse enhanced spectrum is in the range 1300 to 1900 km s^{-1} . Clearly, the principal spectrum is closer to the observed expansion velocity of the nebula at $490 \pm 20 \text{ km s}^{-1}$ (Gill & O’Brien, 2000).

In order to obtain an estimate for what the principal velocity is, we take the two relations that relate t_3 to $v_{\text{principal}}$ and v_{diffuse} (e.g., Warner, 1989) and relate the two velocities. The $1800 \pm 200 \text{ km s}^{-1}$ observed for the emission lines, then corresponds to a principal spectrum of $900 \pm 150 \text{ km s}^{-1}$.

We leave the velocity as a free parameter and let it vary from 750 km/sec to 2000 km/sec , corresponding to the complete range of possible velocities, without actually any prejudice for or against which spectral velocities should be taken. We assume the velocity to be constant with time, which towards the end of the eruption, when small mass outflows are expected (and therefore a smaller observational footprint), can be a bad approximation. We therefore fit the data only to the first month.

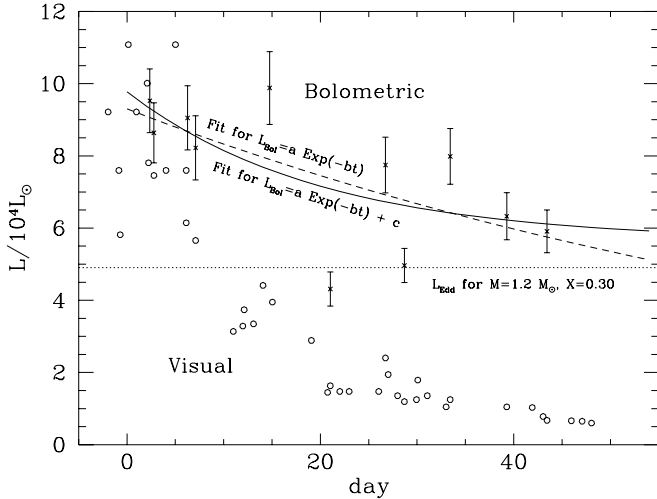


Figure 5. The visual and bolometric luminosity of Nova LMC 1988 #1 taken from Schwarz et al. (1998). Because of the moderate decay rate of the nova, its mass should be of order or less than about $1.2M_{\odot}$. $X = 0.3$ is the typical hydrogen fraction in nova ejecta. The dashed line is a least squares fit to an exponential decay for the bolometric luminosity, giving $L_{\text{bol}} = 9.3 \times 10^4 L_{\odot} \exp(-t/90.5 \text{ days})$. The solid line is the best fit for a luminosity behaviour for an exponential decay plus a constant, giving: $L_{\text{bol}} = 4.13 \times 10^4 L_{\odot} \exp(-t/20.0 \text{ days}) + 5.64 \times 10^4 L_{\odot}$. Evidently, the nova was super-Eddington for a long duration. Unfortunately, adequate measurements of the evolution of the velocity as a function of time do not exist.

Since the observed luminosity exhibits rather large variations, as is apparent in Fig. 5, a smoothed functional behaviour is adopted. A fit of the form $L_{\text{bol}} = a \exp(-bt) + c$ yields the best fit.

Using the wind model and the high load wind relations we find the best \mathcal{W} for a given M_{WD} , X and v_{∞} . The results are found in Fig. 6. Without any prejudice for mass, X or v_{∞} , one finds that the wind model can adequately explain the results with a wind parameter in the range:

$$\mathcal{W}_{\text{LMC}} = 2.8 \pm 1.4. \quad (19)$$

This result is consistent with both the one obtained from Nova FH Serpentis and the one expected from the SEW theory.

3.5 The great eruption of η Carinae

The case of η Carinae is quite different from the novae analyzed. First, the systems are entirely different. Instead of a solar mass type WD, η Car is blue super-giant with a mass of order 60 to $100M_{\odot}$. While the super-Eddington phase of novae lasts of order a few months during which there is a mass loss with a typical rate of $10^{-3} M_{\odot} \text{ yr}^{-1}$, the giant eruption of η Car which started around 1840, lasted for 20 years and has exhibited a mass loss rate of order $10^{-1} M_{\odot} \text{ yr}^{-1}$.

A second difference appears in the way the analysis proceeds. While the novae analyzed had a detailed evolution of the temperature and luminosity, all that we have for η Car is an estimated average luminosity during the 20 year eruption and an estimate for the integrated mass loss. Yet we apply

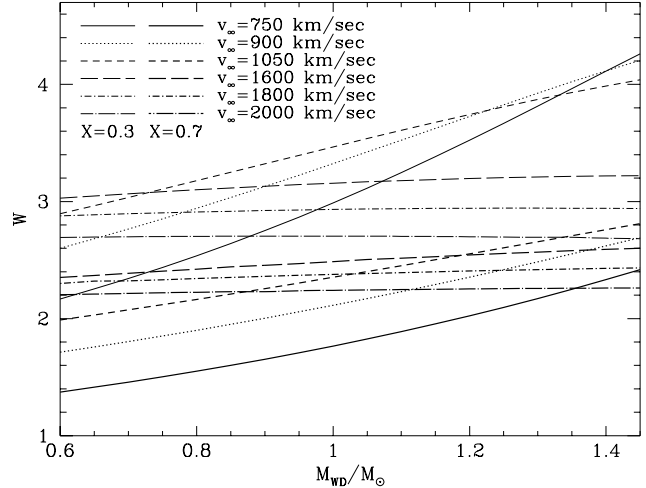


Figure 6. The best fit values of \mathcal{W} for Nova LMC 1988 #1 found for different values of the H mass fraction X and different assumed constant velocity for the outflow, as a function of the assumed WD mass. Values ranging between 1.4 and 4.2 are possible.

the theory and stress that the very same theory is applicable to a wide range of systems.

Following Davidson (1999), we adopt the following parameters for the eruption of η Car: Duration of 20 years. Integrated radiated flux of $10^{49.3 \pm 0.3}$ erg. Ejected mass of 1 to $3M_{\odot}$, and a mass velocity at infinity of 650 km s^{-1} . The mass adopted is $80 \pm 20M_{\odot}$ which can correspond to the estimate of $\sim 60M_{\odot}$ if it is a part of a double star and $\sim 100M_{\odot}$ if it is single.

Using this data, we find that the wind parameter is

$$\mathcal{W} = 4.5 \pm 3.3. \quad (20)$$

The greatest contribution to the error arises from the inaccuracy of the average luminosity while the second largest contribution, which is half the size of the first, comes from the inaccuracy of the mass ejected.

Although the errors in \mathcal{W} are larger than those obtained for Nova LMC 1988 #1, the range obtained from η Car includes entirely the range obtained from Nova LMC 1988 #1. Namely, the results are consistent and the value obtained from Nova LMC 1988 #1 should be taken as the best estimate for \mathcal{W} .

3.6 Possibility of Super-Eddington fluxes

Although we cannot say anything quantitative about the steady state luminosity that will be attained without proper knowledge of the properties of the porous atmosphere, we can understand why super-Eddington fluxes are a natural result.

The steady state luminosity at the post-maximum of novae is generally supposed to be given or at least approximated by the core-mass luminosity relation (CMLR, e.g., Tuchman & Truran, 1998) which describes systems in which a burning shell is situated on an inert (and hence fixed) core (Paczynski, 1970). The CMLR however, saturates at the Eddington luminosity. So, how can it describe cases which were clearly super-Eddington?

A clear physical understanding of the CMLR can be found in Tuchman & Truran (1983) who studied a system composed of an inert core on top of which there is a burning shell, a radiative layer with sharp gradients and a convective layer on top of that. They showed that the conditions above the radiative layer are unimportant for the determination of the burning luminosity (thus, the mass of the envelope is unimportant). Only the burning layer and the radiative layer on top of it affect the luminosity. How would a porous atmosphere change that? Since any inhomogeneities are expected to form in the top part of the atmosphere (above the convective layer), it does not change the analysis of Tuchman & Truran (1983). That is the case only as long as a consistent solution for the top part of the atmosphere is obtainable.

However, as the mass of the WD increases and with it the Eddington parameter, the top part of the atmosphere becomes unstable against formation of inhomogeneous and once these are formed, allows a larger radiative flux for the same average temperature and density gradients. If this larger flux is close enough (or larger than) the Eddington luminosity, the assumption in the analysis of Tuchman & Truran (1983) breaks down because the radiative layer above the burning shell necessarily has to become convective (Joss et al., 1973). Thus, an additional branch for the mass-core luminosity relation becomes possible in which the top part of the atmosphere is inhomogeneous and below it, all the way down to the burning shell, the envelope is convective. Since the luminosity now depends on the photospheric conditions (the convective layer adjusts itself to ‘relate’ the conditions below and on top of it), the core-mass luminosity relation loses its indifference to the parameters of the envelope.

3.7 The ‘Transition Phase’

One of the seemingly odd behaviour that is displayed by a large majority of all the classical nova eruptions is a transition phase. If it appears, it starts once the visual magnitude has decayed by 3 to 4 magnitudes. During the transition phase, the light curve can display strong deepening, quasi-periodic oscillations, erratic changes or other complicated behaviour.

The origin of the transition phase is not clear and it has more than one explanation. For example, the transition phase roughly corresponds to the stage when the photosphere has shrunk to the size of the binary separation such that the companion star can stir up the envelope to produce non trivial behaviour.

The SEW theory naturally introduces another explanation for the transition phase. If we look at the $\Gamma_0 - \dot{W}$ trajectory of Nova FH Serpentis in Fig. 2, one cannot avoid the extrapolation of the trajectory into the zone of ‘no steady state configuration’. What is this region?

The mass loss rate is determined by the luminosity. The mechanism that generates this wind does not depend on whether the luminosity is sufficient or not to carry the material from the sonic point to infinity. If the radius of the sonic point is too small and the escape velocity too high, the wind simply stagnates before leaving the potential well. As predicted by Owocki & Gayley (1997), no steady state solution for the wind exists under such conditions. In other words, the wind model predicts that no steady state could be reached if the radius falls too quickly. This appears to

be a likely scenario in the case of Nova FH Serpentis if one extrapolates its trajectory seen in Fig. 2, and indeed, Nova FH Serpentis was observed to have a transition phase in which the luminosity faded dramatically.

Both the fading and the erratic or quasi-periodic behaviour seem like a natural result here. From Fig. 2, it is apparent that Γ_∞ can fade dramatically before entering the transition phase. This arises from the fact that close to the transition phase almost all of the flux is used to pay for the potential toll. Once in the ‘domain of no steady state’ the non trivial 2D or 3D flows that must result could potentially result with non trivial variability.

The phase is expected to end when the luminosity at the base of the wind falls below the Eddington limit, shutting off the SEW, at which point the ‘naked’ white dwarf should emerge.

3.8 General Mass Loss of Novae

We have previously treated two specific novae for which the temporal evolution of the luminosity and temperature is known in detail. We now turn to describe the nova population in general for which only the average behaviour is known. To do so, we create a template nova as a function of white dwarf mass and explore its properties. Its predicted mass loss is then compared with the observed integrated mass loss. Clearly, we expect the theoretical prediction to provide the guide line to which the *average* behaviour should be compared to.

Let us first estimate the average mass loss in novae. To this goal, we use the average trends for the functional behaviour of the luminosity, decay time and velocity as a function of white dwarf mass to predict the integrated mass loss during the super-Eddington episode. Specifically, we use the following:

(i) We use the average relation between t_3 , the time it takes for the visual luminosity to decay by 3 magnitudes, to the mass of the WD, as is given by Livio (1992).

(ii) We assume that the photospheric velocity is given by the velocity of the principal spectrum. This velocity has an average relation to the decay time t_3 , as given for example by Warner (1989).

(iii) We take the peak bolometric luminosity to be the peak visual luminosity. This is permissible since novae’s maxima are generally in the visual. M_v is related to t_3 , and therefore to M_{WD} , by relations given by Livio (1992). Using M_{WD} , v_∞ and Γ_∞ , we find the Eddington parameter Γ_\star at the base of the wind during the peak brightness. We do so using the relations given in section 2.3.

(iv) We assume that the bolometric luminosity at the *base* decays exponentially (or the magnitude linearly). That is, it has the form: $L(t) = \Gamma_0 \mathcal{L}_{\text{Edd}} \exp(-t/\tau)$. Since we expect the transition phase to arise when the luminosity approaches the Eddington luminosity, and since the transition phase usually sets in after the visual decayed by 3 to 4 magnitudes, or about 3.5 on average, we can relate t_3 to the exponential decay constant of the base luminosity τ :

$$\tau \approx \frac{(3.5/3)t_3}{\ln(\Gamma_0)}. \quad (21)$$

Few words of explanation are in order. It is conceivable that

as the nova eruption proceeds, since the amount of fuel is fixed and all of it burns simultaneously, we do not get a strict steady state cigar-type burning and fixed bolometric luminosity. The bolometric luminosity must change gradually with time. It is customary to assume as a first approximation that $L_{\text{bol}} = \text{constant}$ (Bath & Shaviv, 1976). However, a more realistic treatment that more accurately describes the observations, is to assume a gradual, though slow, decline expressed as an exponential decay with a long time scale (see for instance Fig. 5). For comparison, we also repeat the whole calculation using a linear decline of the form $L(t) = \Gamma_0 \mathcal{L}_{\text{Edd}}(1 - t/\tau)$ and show that the exact form of decay is not critical.

(v) If we integrate the mass loss rate given by the wind theory (eq. 5), we find that the total ejected material during the super-Eddington episode is:

$$\begin{aligned} M_{\text{ejecta}} &= \int_0^{t_E} \dot{M} dt = \frac{\mathcal{W}}{c v_s} \int_0^{t_E} (L - \mathcal{L}_{\text{Edd}}) dt \\ &\approx \frac{\mathcal{W}}{c v_s} \mathcal{L}_{\text{Edd}} \tau (\Gamma_0 - 1 - \ln(\Gamma_0)), \end{aligned} \quad (22)$$

where t_E is the time it takes the bolometric luminosity to decline to the Eddington one.

The results are plotted in Fig. 7 as a function of the mass of the white dwarf, together with the observed determinations of ejecta masses, as was compiled by Hack *et al.* (1993). We first notice that in those cases where multiple determinations were obtained, there are large differences between measurements. These differences should therefore be taken as the typical ‘error’ in cases where only one determination was performed. The different theoretical predictions correspond to changing the wind parameter \mathcal{W} to within the possible range of 2.8 ± 1.8 , when assuming a linear instead of an exponential decay, and when taking into account the natural scattering in the $t_3 - M_{\text{WD}}$ relation of Livio (1992).

To within the large uncertainties of ejecta mass determinations (which have a $1 - \sigma$ scatter of 0.54 dex), the prediction and observations appear to be in good agreement. The super-Eddington episode of novae could account for the bulk, if not all, of the ejected material as a function of M_{WD} . One should nevertheless note that the logarithmic average of the observations: $\langle \log_{10}(M_{\text{ejecta}}/M_{\odot} \text{ yr}^{-1}) \rangle = -4.40 \pm 0.09$ is on the upper side but still within the allowed region predicted by the SEW theory (which has only a small functional dependence on M_{WD}). Since some of the ejecta mass determinations are susceptible to clumpiness, taking the latter into account should tend to reduce the logarithmic average. If $\delta \approx 3$ is a typical value and if a half of the measurements actually measure $M_{\text{ejecta}}\delta$, then the average of the mass loss would be smaller by about a 0.25 dex.

Several additional conclusions can be drawn from Fig. 7. The plateau in the predicted mass loss, where the mass loss does not depend on the mass of the white dwarf, extends from $M_{\text{WD}} = 0.5M_{\odot}$ to $1.2M_{\odot}$. This appears to agree with observations. Moreover, the extrapolation to WD masses beyond $1.2M_{\odot}$ agrees with the mass loss observed from the very fast nova V1500 Cygni, however, this extrapolation should be done cautiously because the assumption of a steady state wind is not strictly valid.

The plateau predicted by the SEW and seen in the ob-

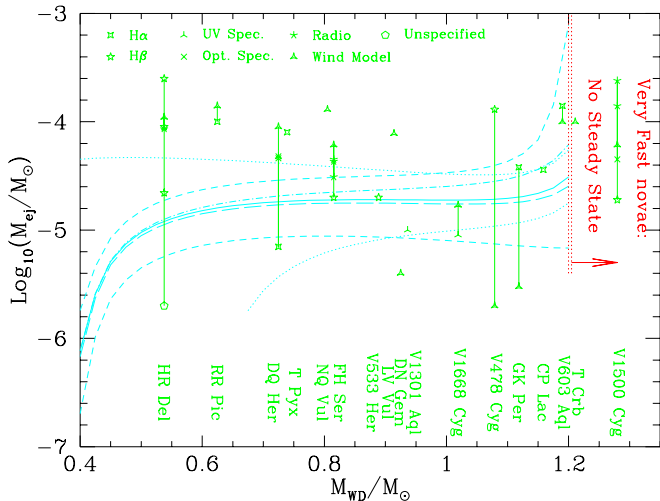


Figure 7. Nova ejected shell mass vs. mass of WD. The symbols describe the measured mass loss for different observed novae as compiled by Hack *et al.* (1993). Large measurement errors are apparent in cases where more than one measurement exists (in which case a vertical line connects the points). One should also note that some measurements overestimate the mass loss when the wind is clumpy, as it is predicted to be. The solid line describes the mass loss obtained by the wind model assuming a nominal value of $\mathcal{W} = 2.8$ as obtained from Nova LMC 1988 #1, following the description in the text. The long dashed line is obtained when changing the Hydrogen mass fraction from 0.7 to 0.3. The upper (and lower) short dashed lines are obtained when taking a value for \mathcal{W} which is higher (lower) by 1.5, while the dash-dotted line arises when the assumed exponential decay is replaced by a linear decay. The dotted lines arise when taking into account the natural scatter in the $t_3 - M_{\text{WD}}$ relation obtained by Livio (1992).

servations is counter to theoretical predictions of the TNR process in which the general trend should be a smaller mass loss with larger WD masses. This theoretical trend arises from the fact that more massive WDs are more compact and ignite the TNR after significantly less material is accreted. For some reason, this trend is not seen. The current theory of novae tends to predict values which are about half an order to an order of magnitude smaller than the typical observations for large WD masses (e.g., Starrfield, 1999, Pringle & Kovetz, 1995, Starrfield *et al.*, 1998). The implementation of the SEW theory in numerical simulations of thermonuclear runaways is now underway with the purpose of finding the luminosity at the base of the wind self consistently as well as to see to what extent the incorporation of the SEW reduces or even eliminates, the difference in ejected mass between the observations and TNR simulations.

3.9 A ‘Constant Bolometric Flux’

Let us return to Fig. 2. Recall that lines of constant radius are close to being vertical. one can see that for moderately ‘loaded’ winds and Γ_* of a few, an evolution in which the temperature increases but the apparent luminosity remains constant is possible if the radius does not decrease dramatically. Under such conditions, the luminosity at the base of the wind does fall off to get a higher and higher temperature, however, the lower mass loss predicted implies that

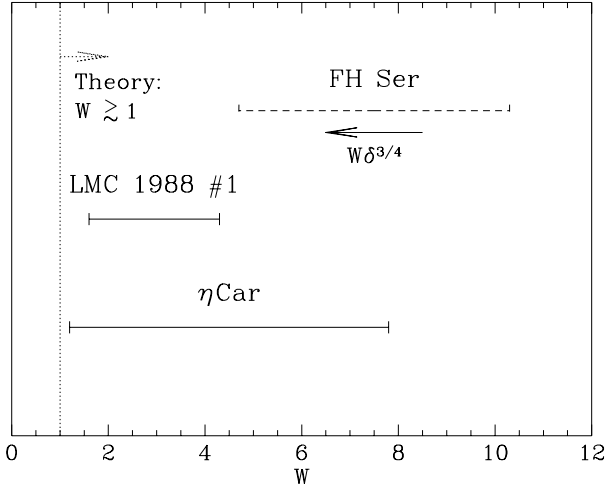


Figure 8. The wind parameter obtained from three independent objects. In the case of FH Ser, the result $W\delta^{3/4}$ is an upper limit since any clumpiness in the wind will mimic a larger inferred value for W if homogeneity (i.e., $\delta = 1$) is assumed. Since the wind is expected to be clumpy, the larger value obtained is a good indication that the analysis and the model are consistent.

less energy is needed to accelerate the material to infinity and so a larger fraction of the base luminosity remains after the wind has been accelerated.

This could explain for example the constant bolometric luminosity observed for V1974 Cygni 1992 (Shore et al., 1994) and supports the early claims (Bath & Shaviv, 1976, Gallagher & Starrfield, 1976) that novae evolve with a bolometric luminosity which is almost constant, or at least one that does not vary dramatically.

Interestingly, depending on the load of the wind, the constant apparent bolometric flux can be either super or sub-Eddington. That is, even if an apparent sub-Eddington luminosity is observed, the system could still have been super-Eddington over dynamically long durations. Under such cases, the kinetic and potential energies of the flow are important.

3.10 Clumpiness of the wind

Clumpiness was already mentioned on several occasions. Since it is important, it deserves a more concentrated discussion.

SEWs are expected to be *always* clumpy as they are generated by an inhomogeneous atmosphere. The results for $W\delta^{3/4}$ for Nova FH Serpentis as compared to the results for W of Nova LMC 1988 #1 do indicate that the winds are clumpy and that the clumpiness factor could be similar to that already observed in the optically thick winds of Wolf-Rayet stars, namely, $\delta \sim 3$. This can be seen in Fig. 8 which depicts the W obtained in the three discussed systems.

Clumpiness is also important because it tends to offset the estimates for the mass ejected from novae and other objects by overestimating it. This arises because many emission processes are more efficient at higher densities. For example, the opacity per unit mass of free-free emission is proportional to ρ . Thus, if the material is clumpy, then the higher

density material is more efficient at producing the observed radiation and while appearing to fill the same volume.

What is the expected size of the clumps? Since they originate from the inhomogeneities at the base of the wind, one should know what the typical size d of the atmospheric perturbations is at this point. For the instabilities found to operate in Thomson scattering atmosphere (Shaviv, 2000a), the typical size is a few times the size of the pressure scale height h (say, αh). As the wind expands from its base, the clumps will keep their angular extent relative to the star. Thus, the spherical harmonic ℓ at which the structure should peek should be of order:

$$\ell \approx 2\pi \frac{R}{d} = 2\pi \frac{R}{\alpha h} \approx \frac{\pi(1 - \Gamma_{\text{eff}}) v_{\text{esc}}^2}{\alpha v_s^2}, \quad \alpha \gtrsim O(1) \quad (23)$$

where v_s is the speed of sound at the base of the wind, which is higher than that at the photosphere. The typical number obtained for nova, is $\ell \sim 1000$. This is a large number and it implies that the ejecta has many small clumps in it. Since the perturbations are expected to be dynamic and change over a sound crossing time, their vertical extent should be of order $v_{\infty} \alpha h$ or more, at large distances, after the velocity dispersion had time to disperse the blobs vertically. (The horizontal dispersion arising from velocities of order of the speed of sound are not important because of the horizontal expansion induced by rarefaction in the spherical geometry).

4 DISCUSSION & SUMMARY

The existence of steady state super-Eddington outflows is an observational fact. One therefore needs to explain on one hand how atmospheres can sustain a super-Eddington state and on the other, one needs to understand the winds that they will generate.

We have tried to present the following coherent picture: Homogeneous atmospheres becomes inhomogeneous as the radiative flux approaches the Eddington limit. This is due to a plethora of instabilities. The particular governing instability depends on the details of the atmosphere. As a consequence of the inhomogeneity, the effective opacity is reduced as it is easier for the radiation to escape, and consequently, the effective Eddington limit increases.

Super-Eddington configurations are now possible because the bulk of the atmosphere is effectively sub-Eddington. Very deep layers advect the excess total luminosity above Eddington by convection. Higher in the atmosphere, where convection is inefficient, the Eddington limit is effectively increased due to the reduced effective opacity. The top part of the atmosphere, where perturbations of order of the scale height become optically thin, has however to remain super-Eddington. Thus, these layers are pushed off by a continuum driven wind.

By identifying the location of the critical point of the outflow, one can obtain a mass-loss luminosity relation. The relation, given by eq. (5) is the main result of the paper. Adding to eq. (5) the basic results for optically thick winds eq. (10) (Owocki & Gayley, 1997) and eq. 14 (Bath & Shaviv, 1976) or eq. (15) (Bath, 1978), we are left with one free universal dimensionless parameter which should be of order or somewhat larger than unity.

To check the result, we analyze 2 novae as well as the

massive star η Carinae. Although the two types of systems are markedly different, as they have masses, luminosities and mass loss rates which differ by orders of magnitude, the wind mass loss and the wind parameter are found to be in agreement with the theoretical expectation:

$$\dot{M} = \mathcal{W} \frac{\mathcal{L}_{Edd}}{cv_s} (\Gamma - 1), \text{ with } \mathcal{W} = 2.8 \pm 1.4. \quad (24)$$

The evolution of the temperature predicted from the luminosity agrees well with the temperature measured directly in the two novae.

Another interesting agreement is the consistency with clumping. Clumping in SEWs is a natural prediction since the atmospheric layers beneath the sonic point are predicted to be inhomogeneous. Moreover, clumpiness is a necessary ingredient in the present theory that allows super-Eddington luminosities. The present theory predicts therefore that SEWs are clumpy. In the analysis of Nova FH Serpentis, the wind parameter obtained is coupled to the clumpiness of the wind since a clumpy wind with the same observed colour temperature will have a lower inferred mass loss. The lower \dot{m} reduces the measured wind parameter towards that obtained for Nova LMC 1988 #1 when the typical clumpiness factors seen in WR winds are taken into account.

We identify the occurrence of the ‘transition phase’ observed in more than 2/3 of the novae with the advance of the atmosphere into the ‘no steady state region’. As the nova explosion progresses, its luminosity and radius decline. However, if the radius decreases too quickly, at some point the SEW predicted will be too heavy for the luminosity at the base to push to infinity. No steady state will then exist. The inconsistency might explain the strange behaviours observed in the transition phase of different novae.

The wind model presented is by no means a complete theory for novae since it cannot predict *ab initio* the luminosity at the base of the wind. To obtain the latter, one needs to solve for the complete evolution of a nova taking into account the fact that the nova’s atmosphere becomes porous and have a reduced lowered opacity. One expects that the lowered opacity increases the luminosity obtained in the core-mass luminosity relation, and super-Eddington values therefore arise naturally.

In order to fully understand the behaviour of the atmosphere that drives these winds, a 2D or even 3D numerical simulations on scales of the order of few optical depths are unavoidable because of the intrinsic nonlinear properties of the problem. These simulations are underway.

ACKNOWLEDGMENTS

The author would like to thank useful comments from Stan Owocki and Ken Gayley and CITA for the fellowship supporting him.

REFERENCES

- Arons J., 1992, ApJ, 388, 561
 Bath G. T., 1978, MNRAS, 182, 35
 Bath G. T., Shaviv G., 1976, MNRAS, 175, 305
 Castor J. I., Abbott D. C., Klein R. I., 1975, ApJ, 195, 157

- Davidson K., 1999, in Morse J. A., Humphreys R. M., Daminieli A., eds, ASP Conf. Ser. 179: Eta Carinae at The Millennium, p. 6
 Davidson K., Humphreys R. M., 1997, ARA&A, 35, 1
 della Valle M., Gilmozzi R., Bianchini A., Esenoglu H., 1997, A&A, 325, 1151
 Duerbeck H. W., 1992, Acta Astronomica, 42, 85
 Friedjung M., 1987, A&A, 179, 164
 Friedjung M., 1989, in Bode M. F., Evans A., eds, Classical Novae, John Wiley & Sons, Oxford
 Gallagher J. S., Code A. D., 1974, ApJ, 189, 303
 Gallagher J. S., Starrfield S., 1976, MNRAS, 176, 53
 Gill C. D., O’Brien T. J., 2000, MNRAS, 314, 175
 Glatzel W., Kiriakidis M., 1993, MNRAS, 262, 85
 Hack M., Selvelli P., Duerbeck H. W., 1993, Cataclysmic Variables and Related Objects (N95-27068 09-89), NASA, Washington, p. 261
 Joss P. C., Salpeter E. E., Ostriker J. P., 1973, ApJ, 181, 429
 Kato M., Hachisu I., 1994, ApJ, 437, 802
 Livio M., 1992, ApJ, 393, 516
 Owocki S. P., Gayley K. G., 1997, in Nota A., Lamers H., eds, ASP Conf. Ser. 120: Luminous Blue Variables: Massive Stars in Transition, p. 121
 Paczynski B., 1970, Acta Astronomica, 20, 47
 Paresce F., Livio M., Hack W., Korista K., 1995, A&A, 299, 823
 Pauldrach A., Puls J., Kudritzki R. P., 1986, A&A, 164, 86
 Prialnik D., 1986, ApJ, 310, 222
 Prialnik D., Kovetz A., 1995, ApJ, 445, 789
 Schwarz G. J., Hauschildt P. H., Starrfield S., Whitelock P. A., Baron E., Sonneborn G., 1998, MNRAS, 300, 931
 Schwarz, et al., 2000, preprint
 Shaviv N. J., 1998, ApJ, 494, L193
 Shaviv N. J., 2000a, submitted to ApJ
 Shaviv N. J., 2000b, ApJ, 532, L137
 Shore S. N., Sonneborn G., Starrfield S., Gonzalez-Riestra R., Polidan R. S., 1994, ApJ, 421, 344
 St.-Louis N., Moffat A. F. J., Lapointe L., Efimov Y. S., Shakhovskoj N. M., Fox G. K., Piirola V., 1993, ApJ, 410, 342
 Starrfield S., 1999, Phys. Rep., 311, 371
 Starrfield S., Truran J. W., Wiescher M. C., Sparks W. M., 1998, MNRAS, 296, 502
 Stothers R. B., Chin C., 1993, ApJ, 408, L85
 Tuchman Y., Truran J. W., 1998, ApJ, 503, 381
 Tuchman Y., Glasner A., Barkat Z., 1983, ApJ, 268, 356
 Warner B., 1989, in Bode M. F., & Evans A., eds, Classical Novae. John Wiley & Sons, Oxford